# Nuclear localization or inclusion body formation of ataxin-2 are not necessary for SCA2 pathogenesis in mouse or human

Duong P. Huynh, Karla Figueroa, Nam Hoang & Stefan-M. Pulst

**Instability of CAG DNA trinucleotide repeats is the mutational mechanism for several neurodegenerative diseases resulting in the expansion of a polyglutamine (polyQ) tract. Proteins with long polyQ tracts have an increased tendency to aggregate, often as truncated fragments forming ubiquitinated intranuclear inclusion bodies. We examined whether similar features define spinocerebellar ataxia type 2 (SCA2) pathogenesis using cultured cells, human brains and transgenic mouse lines. In SCA2 brains, we found cytoplasmic, but not nuclear, microaggregates. Mice expressing ataxin-2 with Q58 showed progressive functional deficits accompanied by loss of the Purkinje cell dendritic arbor and finally loss of Purkinje cells. Despite similar functional deficits and anatomical changes observed in ataxin-1[Q80] transgenic lines, ataxin-2[Q58] remained cytoplasmic without detectable ubiquitination.**



## Introduction

SCA2 belongs to the growing family of neurodegenerative diseases caused by expansion of a polyQ tract. This group now includes SCA1 (ref. 1), Machado-Joseph disease[2] (SCA3 or MJD), SCA6 (ref. 3), SCA7 (ref. 4), Huntington disease[5] (HD), spinal bulbar muscular atrophy[6] (SBMA) and dentatorubral pallidoluysian atrophy[7] (DRPLA). Despite their phenotypic differences, evidence has suggested that these diseases share a common pathogenetic mechanism. To some degree, polyQ diseases can be regarded as prototypes of human neurodegenerative diseases caused by mutant and misfolded proteins. Although ubiquitination, intranuclear location of full-length or truncated proteins and caspase cleavage have all been implicated in polyQ pathogenesis, it is not clear which features are common to polyQ diseases or which features are necessary and sufficient for pathogenesis.

Because intranuclear aggregates are found in a subset of neurons in the brains of patients with SCA3 and HD, it has been suggested that formation of intranuclear inclusions (NIs) is a common feature causing polyQ-mediated neuronal death. NIs were also found in mouse models of human polyQ diseases and in cultured cells when they were transfected with cDNAs containing long CAG repeats[8–17]. Several studies, however, have questioned their importance for pathogenesis. Transgenic mouse lines expressing a truncated amino-terminal huntingtin fragment with more than 130 glutamine repeats had an abundant number of NIs, but there was little evidence for a role for NIs in neurodegeneration[13]. In contrast, mice expressing full-length huntingtin with either 48 or 89 glutamine repeats exhibited striatal neuronal death with few NIs in these neurons[18]. *In vitro* studies with huntingtin showed that nuclear localization of the mutant protein was required for neurodegeneration[15], but the formation of the NIs did not correlate with neuronal death induced by mutant huntingtin[19–21]. In addition, although intranuclear aggregates are found in HD brains, most polyQ aggregation in HD is perinuclear[20,21]. On the other hand, for SCA1 pathogenesis, intranuclear location of ataxin-1 was necessary for pathogenesis, although the formation of aggregates was not[22].

Some NIs show co-localization with ubiquitin, proteasomal proteins or heat-shock proteins[8–17], suggesting degradation by the ubiquitin-proteasome pathway. The importance of ubiquitination has recently been demonstrated for ataxin-1. Lack of one of the crucial enzymes in ubiquitination, the Ube3 ligase, resulted in decreased inclusions, but increased severity of Purkinje cell pathology in mouse transgenic lines[23]. It is unknown whether targeting by the ubiquitin-proteasomal pathway is a common feature of all mutant polyQ proteins, and ataxin-6 did not appear to be ubiquitinated in human SCA6 brains[24].

The protein product of *SCA2*, designated ataxin-2 (Fig. 1), is composed of 1,312 amino acid residues with a calculated molecular weight of 140 kD. The most common form of wild-type ataxin-2 contains 22 glutamine repeats flanked by a region of proline- and serine-rich domains. In contrast, mouse ataxin-2 has only one glutamine at the site of the human polyQ tract[25], suggesting that the normal function of ataxin-2 resides in the regions flanking the CAG repeat. With expansion of the polyQ tract to 34 or more, individuals will develop the SCA2 phenotype. Except for the CAG trinucleotide expansion, the protein product of *SCA2* has no similarity with other polyQ proteins[1–7,26–28]. Immunohistochemical studies found that ataxin-2 had a cytoplasmic location in normal brain and was expressed in Purkinje cells and specific groups of brainstem and cortical neurons[29]. Ubiquitinated NIs have been found only in 1–2% of pontine neurons of SCA2 patients, but not in Purkinje cells, which are the primary target in SCA2 pathology[30].

Although the study of normal and diseased human brains can provide important insights into polyQ pathogenesis, such observations are limited to the terminal stages of the disease process. Mouse models can circumvent this problem, but many mouse models of human polyQ diseases rely on the use of truncated constructs or very long polyQ tracts to produce neurodegeneration[31–34]. In addition, several polyQ mouse models do not show prominent neuronal cell loss, a defining feature of human polyQ diseases. Here we provide evidence that SCA2 pathogenesis does not require intranuclear localization of the protein and that

*Rose Moss Laboratory for Parkinson's and Neurodegenerative Diseases, CSMC Burns and Allen Research Institute, and Division of Neurology, Cedars-Sinai Medical Center, UCLA School of Medicine, Los Angeles, California, USA. Correspondence should be addressed to S.-M.P. (e-mail: Pulst@CSHS.org).*

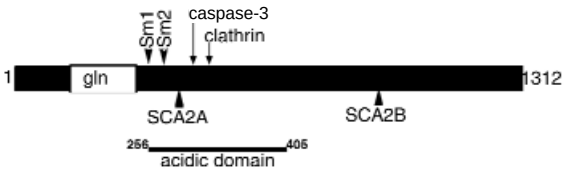


**Fig. 1** Schematic map of ataxin-2. Ataxin-2 is a protein with 1,312 aa. Within the acidic domain lie two RNA-binding motifs, the Sm1 and Sm2 sites at aa 230–233 and aa 283–286, respectively, a putative caspase-3 recognition site at aa 396–399, and a clathrin-mediated sorting signal at aa 414–416 downstream of an ER exit signal. The predicted MW for the caspase-3 cleavage ataxin-2 product is 41.2 kD. Antibodies were generated against two peptides, SCA2A and SCA2B, the location of which is indicated.

mutant ataxin-2 does not form large aggregates or inclusion bodies. Mouse lines expressing mutant ataxin-2 show functional and morphological deficits similar to those of mouse lines expressing mutant ataxin-1 (refs 35–37), but without nuclear localization or a detectable increase in ubiquitin-conjugated protein complexes.

## Results

### Lack of intranuclear inclusion bodies in SCA2

We previously reported that ataxin-2 had a cytoplasmic localization in three brains from SCA2 patients[29]. It was possible, however, that ataxin-2 was processed to smaller polyQ-containing fragments that did not include the epitope recognized by our ataxin-2 antibodies. To address this, we used the 1C2 monoclonal antibody, which recognizes expanded polyQ repeats. We analysed the presence of ataxin-2 fragments by western-blot analysis of brain protein extracts from an SCA2 patient (Fig. 2*a*, lane 1), a neurologically normal individual (Fig. 2*a*, lane 2) and an Alzheimer patient (Fig. 2*a*, lane 3). Western blots were stained with the SCA2A and SCA2B antibodies, and compared with the pattern observed by staining the identical extracts with the 1C2 monoclonal antibody. The SCA2A antibody recognized full-length ataxin-2 with the normal (145 kD) and expanded polyQ repeats (180 kD), as well as a 42-kD fragment in the SCA2 patient (Fig. 2*a*, lane 1). The 42-kD protein was barely detectable in normal brain or Alzheimer brain. As expected, the 1C2 antibody recognized the 180-kD fragment but not the 145-kD protein; it also recognized the 42-kD fragment in the SCA2 patient. This fragment was barely detected by the 1C2 antibody in the Alzheimer and control brains. The 1C2 antibody did not detect smaller proteins of significant abundance, indicating that the 42-kD protein was the smallest fragment containing an expanded polyQ tract.

To further confirm that the 42-kD fragment was generated preferably by ataxin-2 with an expanded polyQ tract, and to investigate whether mutant ataxin-2 was ubiquitinated, we transfected 293T cells with pEGFP-SCA2[Q22] or pEGFP-SCA2[Q58], followed by treatment with lactacystin for 24 hours to inhibit the proteasomal pathway. Untreated cells served as controls. We performed western blots on these protein extracts and insoluble pellets using the GFP or ubiquitin antibody (Fig. 2*b*). The GFP antibody detected the full-length GFP–ataxin-2 with Q22 and Q58 at 200 kD, and an additional band at 70 kD in 293T cells transfected with pEGFP-SCA2[Q58] (Fig. 2*b*, lanes 3, 4). Neither the 70-kD nor the 200-kD proteins were detected in untransfected 293T protein extracts (Fig. 2*b*, lanes 5, 6). The 70-kD protein was not abundant in the pEGFP-SCA2[Q22] transfected cells (Fig. 2*b*, lanes 1, 2), suggesting that the 42-kD fragment was preferably generated from ataxin-2 containing expanded polyQ repeats.

Treatment with lactacystin irreversibly inhibits the proteasomal pathway resulting in the accumulation of ubiquitin-conjugated protein complexes. The ubiquitin antibody detected a strong smear above 60 kD in protein extracts of lactacystin-treated cells compared with untreated samples, indicating that lactacystin treatment had caused a general increase in ubiquitin-conjugated protein complexes in 293T cells (Fig. 2*b*,*c*). There were no large aggregates above the p200 band detected by the GFP antibody in either the control or the lactacystin-treated cells. Western blots of detergent-insoluble and nuclear proteins from these cells with either GFP or SCA2 antibodies did not detect any additional large protein complexes (Fig. 2*b*,*c*). The levels of both GFP–ataxin-2[Q22] and GFP–ataxin-2[Q58] fusion proteins were increased in the insoluble fractions of the lactacystin-treated transfected cells (Fig. 2*b*, lanes 8, 10), suggesting that GFP–ataxin-2 might decrease ataxin-2 solubility. To investigate whether the GFP fusion caused any interference with ubiquitin conjugation, we transfected 293T cells with pcDNA-SCA2[Q22] or pcDNA-SCA2[58] and treated them with lactacystin. Western blots of these protein extracts with 1C2 or ubiquitin antibodies showed that lactacystin treatment increased the total amount of ataxin-2[Q58] (p180), but no large ataxin-2 aggregates were found (Fig. 2*c*, lanes 3, 4). In the insoluble fractions, ataxin-2[Q58] was faintly detected in both lactacystin-treated and untreated samples (Fig. 2*c*, lanes 9, 10), suggesting that the full-length ataxin-2[Q58] without GFP fusion was detergent soluble. These results showed that there were no detectable large ubiquitin-conjugated protein complexes formed by mutant ataxin-2, although polyQ expansion resulted in an accumulation of ataxin-2 that was enhanced by lactacystin treatment.

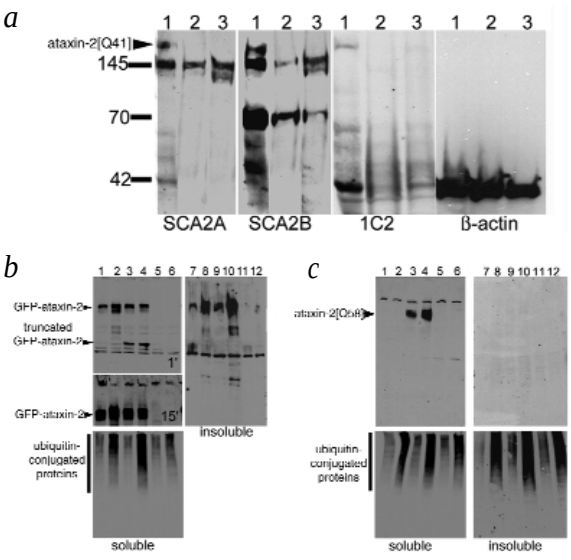


**Fig. 2** Expression of ataxin-2. ***a***, Western blot of human cortical brain extracts probed with antibodies to ataxin-2 peptides (SCA2A and SCA2B), 1C2 (to polyQ domains) and β-actin. We loaded 100 μg brain protein extracts from an SCA2 patient (lane 1), normal individual (lane 2) and Alzheimer patient (lane 3) per lane. Both ataxin-2 antibodies detected full-length ataxin-2 (145 kD) in all three extracts, and a full-length ataxin-2[Q41] (180 kD) in the SCA2 extract (lane 1). The SCA2A antibody also detected a 42-kD fragment that was recognized by the 1C2 antibody. The SCA2B antibody detected an additional 70-kD protein in all samples (panels for antibodies SCA2A and SCA2B were previously shown[29]). ***b***, Western blot of 293T cells transfected with pEGFP-SCA2[Q22] (lanes 1, 2, 7, 8), pEGFP-SCA2[58] (lanes 3, 4, 9, 10) and controls (lanes 5, 6, 11, 12) detected with antibodies to GFP (top) and ubiquitin (bottom). *b*,*c*, Lanes 1–6 contain soluble proteins and lanes 7–12 contain insoluble proteins. Lactacystin-treated samples were loaded in even-numbered lanes and untreated samples were in odd-numbered lanes. Lactacystin-treated cells had increased levels of ubiquitin-conjugated protein complexes and GFP-tagged ataxin-2. ***c***, Western blot of 293T cells transiently transfected with pcDNA-SCA2[Q22] (lanes 1, 2, 7, 8), pcDNA-SCA2[Q58] (lanes 3, 4, 9, 10) and controls (lanes 5, 6, 11, 12) detected with 1C2 and ubiquitin antibodies.

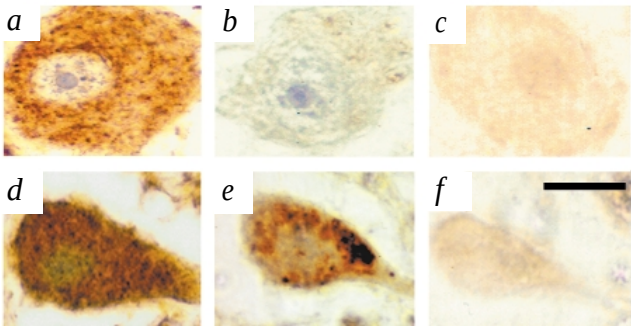


**Fig. 3** Immunohistochemical staining of cerebellar sections from a normal individual (*a–c*) and an SCA2 patient with 58 CAG repeats (*d–f*). We nuclear counterstained with haematoxylin. Purkinje cells were stained with antibodies to ataxin-2 peptides SCA2A (***a***,***g***), the 1C2 monoclonal antibody to polyQ tracts (***b***,***e***) and ubiquitin (***c***,***f***). Bar, 20 μm.

To investigate whether intranuclear inclusion bodies consisting of truncated or ubiquitinated ataxin-2 fragments were abundant *in vivo* in human SCA2 tissues, we used antibodies to ataxin-2 (SCA2A), the polyQ tract (1C2) and ubiquitin to stain sections from a normal cerebellum and the cerebellum from an SCA2 patient with 58 CAG repeats. As previously shown[29], the SCA2A antibody staining was strong, punctate and evenly distributed in normal Purkinje cells (Fig. 3*a*), whereas the 1C2 antibody failed to label any cellular structures (Fig. 3*b*). Ubiquitin labelling was undetectable in Purkinje cells and other neurons in both normal and SCA2 brain sections (Fig. 3*c*,*f*). The same ubiquitin antibody detected Lewy bodies in the midbrain of two patients with sporadic Parkinson disease (data not shown) and a smear banding pattern in the lactacystin-treated 293T cells (Fig. 2*b*,*c*), confirming that this antibody detects ubiquitin-conjugated protein complexes. Moreover, antibodies to proteasomal subunits did not show enhanced labelling of Purkinje cells or other neurons in SCA2 brain sections (data not shown). In brain sections from four different SCA2 brains, both the SCA2A and 1C2 antibodies labelled Purkinje cells (Fig. 3*d*,*e*) throughout the cytoplasm with some granulated cytoplasmic vesicles (Fig. 3*d*). The 1C2 antibody did not label normal Purkinje cells (Fig. 3*b*), but did intensely label large cytoplasmic structures in SCA2 Purkinje cells (Fig. 3*e*).

## Transgenic mouse lines expressing mutant ataxin-2

Because intranuclear inclusions have been identified in all animal models of human dominant ataxias so far[18,22,32–36], we investigated the effect of expression of full-length *SCA2* cDNA under the control of the Purkinje-cell–specific Pcp2 regulatory element[37] (Fig. 1) on morphology and function of Purkinje cells. We evaluated three lines expressing ataxin-2[Q58] and two lines expressing ataxin-2[Q22]. Quantitative Southern-blot analysis of *Rsa*I-digested DNA showed that there were two transgene copies for line Q58-5B, and three or four copies for lines Q58-11 and Q58-19, whereas lines Q22-4 and Q22-5 had one copy each. In contrast to human expanded *SCA2* CAG repeats, which are unstable and continue to expand in succeeding generations[27], 45 offspring in 3 generations of the Q58-11 line transmitted the transgene stably (data not shown).

To determine whether the transgenes were expressed, we extracted RNA and protein from cerebella of transgenic lines. mRNA was reverse transcribed into single-strand DNA. An aliquot of the reaction was subjected to PCR using human-specific primer pairs spanning the CAG tract. Cerebella of transgenic mice, but not of wild-type mice contained transgene mRNA with either $CAG_{22}$ or $CAG_{58}$ (Fig. 4*a*).

Western-blot analysis of protein extracts isolated from the cerebella of Q58-11 mice demonstrated expression of the transgenes at the protein level. We detected a 180-kD protein in the cerebella from Q58-11 heterozygous and homozygous mice with the expected increased expression in homozygous animals (Fig. 4*b*). This band was not detected in wild-type animals. Several proteins of smaller molecular weight were seen in wild-type and transgenic lines, suggesting that they were mouse endogenous proteins. In tissue sections, the 1C2 antibody labelled Purkinje neurons from lines Q58-5B, Q58-11 and Q58-19, confirming that these lines expressed the human transgene (Fig. 7).

To further determine the relative expression levels of the ataxin-2 transgenes, we performed RT–PCR on total RNA isolated from cerebella of wild-type and transgenic lines using a primer pair (3014A-3258B) spanning exon 15 and amplifying endogenous and transgene mRNA (Fig. 4*c*). The human and mouse PCR products can be differentiated after digestion with *Mse*I, which cleaves only the endogenous mouse 266-bp PCR product into two fragments of 79 bp and 187 bp. Line Q22-4 had a slightly higher transgene expression than line Q22-5 at levels comparable with heterozygous animals in lines Q58-5B and Q58-19. Transgene expression in line Q58-11 was the highest of all lines. These experiments also demonstrated that transgene

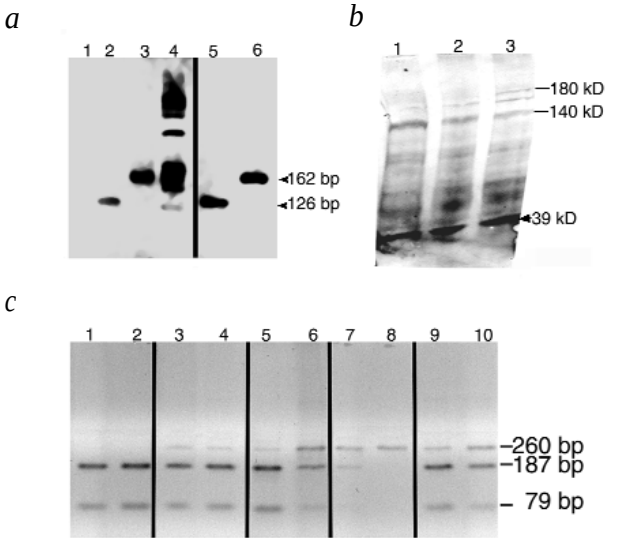


**Fig. 4** Expression of the human ataxin-2 transgene in mice as seen by RT–PCR and western-blot analyses. ***a***, Expression of the SCA2 transgene. Cerebella from a wild-type (lane 1), line Q22-5 (lane 2) or line Q58-11 mouse (lane 3) were subjected to RT–PCR using a human-specific primer pair (A1-B1) flanking the CAG repeat. The A1-B1 primer pair generated a 126-bp amplicon containing 22 CAG repeats in the Q22-5 line (lane 2) and a 162-bp amplicon containing 58 CAG repeats in the Q58-11 line (lane 3). The 126-bp and 162-bp fragments were also observed in the control PCR reaction containing either the transgenic constructs pZ03-SCA2[Q22] (lane 5) or pZ03-SCA2[Q58] (lane 6). Lane 4 contains DNA marker ϕX174RFDNA/*Hae*III. ***b***, Western-blot analysis of mouse protein extracts probed with the SCA2A antibody. Cerebella (including brainstems) from wild-type (lane 1), heterozygous Q58-11 (lane 2) or homozygous Q58-11 animals (lane 3) were homogenized in triple-detergent buffer and 100 μg of the total protein were loaded in each lane. The SCA2-A antibody detected full-length ataxin-2 and a 39-kD protein fragment in all extracts. A weak 180-kD band was detected in the heterozygous mouse protein extract (lane 2). The 180-kD band was more intense in the homozygous mouse brain extract (lane 3). ***c***, Relative expression of transgenes compared with endogenous ataxin-2 expression levels using RT–PCR. In contrast to the human transgene, the mouse amplicon contains a unique restriction site that results in two fragments of 187 and 79 bp after *Mse*I digestion. Lanes 1, 2, wild type; lane 3, heterozygote Q22-4; lane 4, heterozygote Q22-5; lanes 5, 6, heterozygote and homozygote Q58-5B; lanes 7, 8, heterozygote and homozygote Q58-11; lanes 9, 10, heterozygote and homozygote Q58-19. RNase treatment resulted in loss of all amplicons (not shown).

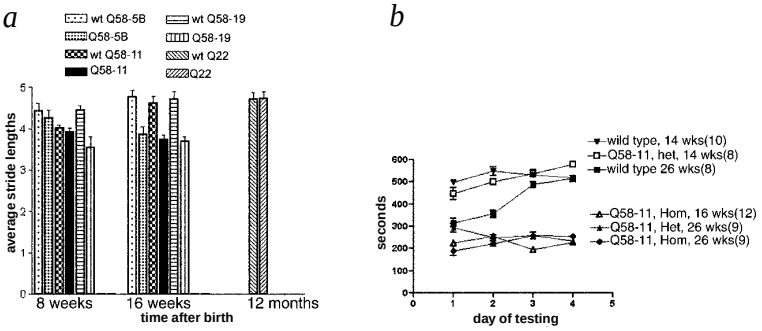


**Fig. 5** Progressive functional loss in lines Q58-5B, Q58-11 and Q58-19. ***a***, Footprint analysis showing progressive reduction in stride length for all three lines examined at 8 and 16 weeks ($n$=11–14 animals per data point). Animals expressing ataxin-2[Q22] have the same stride length as wild-type animals even when examined at 12 months. wtQ58-5B, wtQ58-19 and wtQ58-11 denote wild-type mice matched with the respective transgenic lines. ***b***, Rotarod analysis of mice from line Q58-11. The graph shows average performance on the rotarod apparatus of four trials each day on four consecutive days. Differences were significant for homozygous Q58-11 mice at 16 and at 26 weeks (2-way ANOVA compared with wild type, $P$<0.0001), and for heterozygous Q58-11 mice at 26 weeks ($P$<0.0001). Numbers in brackets indicate number of animals tested.

expression levels in homozygous animals were higher than those in their heterozygous counterparts.

## Functional testing of transgenic lines

We carried out three independent functional tests to determine the effect of transgene expression on Purkinje-cell function: clasping, footprinting and rotarod analysis. Mice with neurodegenerative phenotypes have a tendency to fold their hindlegs when held by the tail for at least one minute. Clasping was observed at 16–20 weeks in line Q58-19 and at 8–12 months in the Q58-11 line. In Q58-5B animals, no clasping was observed up to 26 weeks of age. Q22-4 and Q22-5 animals did not show clasping up to 12 months.

Stride length was altered in mice expressing mutant ataxin-2 compared with that of wild-type mice or mice expressing ataxin-2[Q22] (Fig. 5*a*). In the Q58-19 line, stride length was reduced by 19% at 8 weeks ($P$<0.0001, 2-way ANOVA). At 16 weeks, all 3 Q58 lines showed similar reduction in stride length ($P$≤0.001, 2-way ANOVA). Mice expressing ataxin-2[Q22] showed no significant reduction in stride length compared with wild-type mice, even at 12 months (Fig. 5*a*).

Rotarod testing of lines Q58-11 and Q58-5B confirmed functional deficits. Wild-type, heterozygous and homozygous Q58-11 mice were tested at 6, 14–16 and 26 weeks. At six weeks, motor performance of transgenic animals was not different from that of wild-type mice (data not shown). At 16 weeks, homozygous Q58-11 mice already performed poorly on rotarod testing ($P$<0.001, 2-way ANOVA), whereas heterozygous Q58-11 animals performed as well as wild type (Fig. 5*b*). Although mice from the Q58-5B line exhibited later stride-length deficits than those from the Q58-11 line, their rotarod performance matched that of the Q58-11 mice (data not shown). The functional deficits were progressive. At 26 weeks, both heterozygous and homozygous Q58-11 animals showed severely impaired motor performance. The rotarod performance of animals expressing ataxin-2[Q22] was not significantly different from that of wild-type animals (data not shown).

## Anatomic changes in transgenic lines

To investigate morphological changes in Purkinje cells, we compared calbindin-28K immunoreactivity (IR) in tissue sections from heterozygous animals at 27 weeks with that from wild-type mice. Calbindin-28K is a protein specifically expressed in cytoplasm and dendritic processes of cerebellar Purkinje cells. Most Purkinje cells lost calbindin-28K IR in mice from lines Q58-5B and Q58-11 (Fig. 6*a*,*b*), whereas loss in line Q58-19 was more discreet (Fig. 6*c*). Calbindin-28K loss was progressive (Fig. 6*d*–*i*). At four weeks, calbindin-28K labelling was strong in Q22 mice (data not shown) and wild-type animals (Fig. 6*d*), whereas calbindin-28K IR was already reduced in Purkinje cell bodies of homozygous Q58-11 mice (Fig. 6*g*). From 7 to 14 weeks (Fig. 6*h*,*i*), further loss of calbindin-28K immunoreactivity was observed compared with wild-type animals and Q22 transgenic mice (Fig. 6*e*,*f*,*j*). The loss of calbindin-28K IR in Purkinje cells of Q58-11 mice was similar to that observed in human Purkinje neurons from an SCA2 patient with 41 SCA2 CAG repeats (Fig. 6*l*). Loss of the dendritic arbour was closely followed by a loss in Purkinje cell number. The percentage of surviving Purkinje cells showed a progressive decline. At 24–27 weeks, Purkinje cell number was reduced by 50–53% in lines Q58-5B, Q58-11 and Q58-19. Compared with wild-type mice, mice expressing ataxin-2[Q22] showed no reduction in Purkinje cell number even at one year of age.

Labelling with either the SCA2A or the 1C2 antibody did not reveal NIs. Purkinje cells from all three Q58 transgenic lines

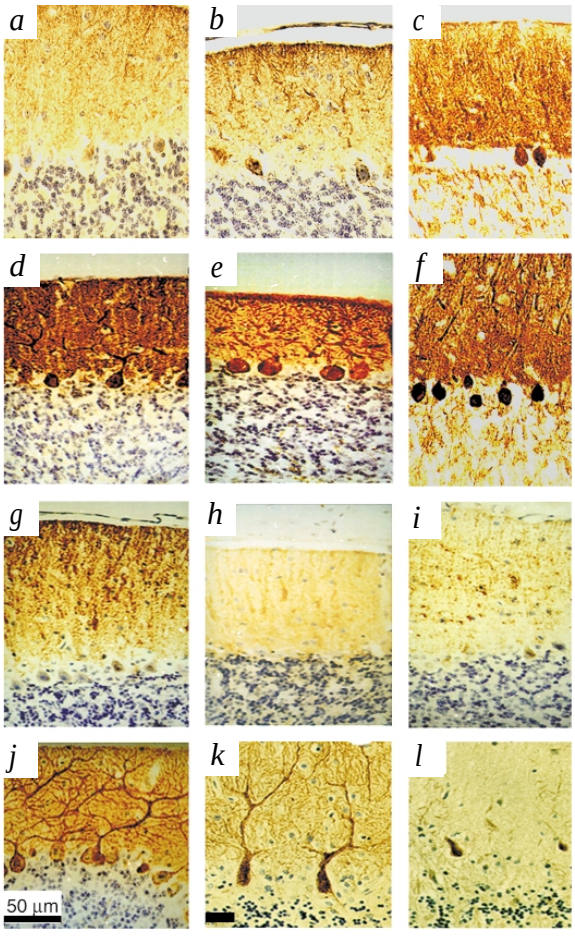


**Fig. 6** Calbindin-28K labelling of cerebella of heterozygous Q58-5B (***a***), Q58-11 (***b***) and Q58-19 (***c***) animals at 27 weeks, and wild-type and homozygous Q58-11 mice at 4 weeks (***d***,***g***), 7 weeks (***e***,***h***) and 14 weeks (***f***,***i***) . A 7-week Q22-5 mouse section (***j***), a human cerebellum from an age-matched normal individual (***k***) and a Q41-SCA2 patient (***l***) are shown for comparison. (*a*–*c*), (*d*–*j*) and (*k*,*l*) were processed simultaneously. Changes in calbindin-28K labelling were seen as early as four weeks but became more pronounced with age. Bar, 50 µm.

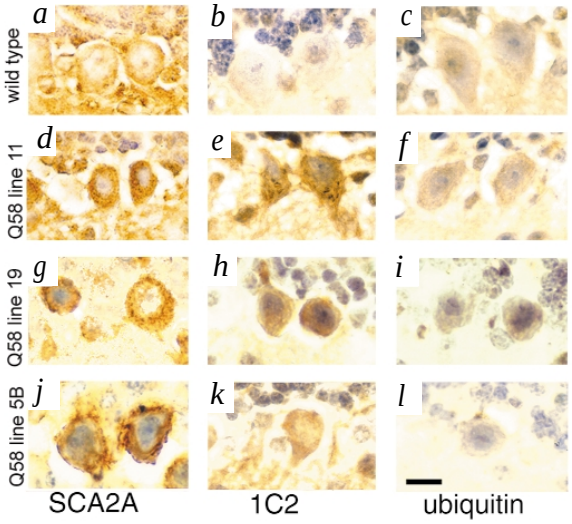


**Fig. 7** Expression and localization of ataxin-2 in Purkinje cells. Paraffin-embedded mouse brain sections from wild-type, Q58-11, Q58-19 and Q58-5B mice were stained with the SCA2A, 1C2 or ubiquitin antibody and counterstained with haematoxylin. Mouse sections shown in (***a***,***b***,***c***,***d***,***e***,***f***); were processed and stained at a different date from those sections in (***g***,***h***,***i***,***j***,***k***,***l***). Note the cytoplasmic accumulation of ataxin-2 immunoreactivity and the lack of nuclear localization in Purkinje cells in the Q58 mouse cerebella (*e*,*f*). Bar, 15 μm.

labelled intensely with the SCA2A and 1C2 antibodies (Fig. 7). The SCA2A staining was more intense than in wild-type Purkinje cells and located throughout the cytoplasm with some granulated cytoplasmic vesicles (Fig. 7). The 1C2 staining consisted of cytoplasmic microaggregates. Ubiquitin labelling was undetectable in Purkinje cells of wild-type and transgenic animals (Fig. 7).

## Discussion

Mouse models of human polyQ diseases have been very instructive in elucidating the morphological and biochemical steps important for pathogenesis. Several unresolved questions involve the subcellular localization of polyQ proteins, their need for aggregation and the importance of truncation in pathogenesis. Our mouse lines share important features with ataxin-1 lines, including the promoter driving the expression of the transgene, the use of full-length cDNAs, and the time course and nature of pathological and functional changes. Despite these similarities, the localization of the respective proteins are very different. This may have important implications for treatment of polyQ diseases.

Lack of NIs. Several mutant proteins that are involved in polyQ diseases form NIs (refs 8–17,19), leading to the hypothesis that intranuclear aggregation of mutant polyQ proteins was a common pathological mechanism for polyQ diseases. This appeared to be correct for both proteins that contain nuclear localization signals (such as ataxin-1) and proteins that lack these signals (such as ataxin-3, which is a cytoplasmic and nuclear protein[10,38]). Ataxin-2 appears to belong to the latter group, in that the protein does not contain any of the known nuclear localization signals and has an exclusively cytoplasmic localization in normal and SCA2 human brain[29].

Evidence from a YAC transgenic model of HD suggested that only truncated N-terminal huntingtin enters the nucleus[39]. Despite this fact, there was little correlation of behavioural deficits with the presence of nuclear N-terminal huntingtin aggregates, suggesting that large nuclear aggregates are unlikely to be causal in HD neurodegeneration, although they may still be important for disease progression[39]. We found evidence of truncation of ataxin-2 in both western blots of brain extracts and cultured cells transfected with full-length ataxin-2[Q58]. The truncated 42-kD fragment contains the polyQ tract, but does not enter the nucleus even when this fragment is overexpressed (data not shown). Because this fragment is recognized by the 1C2 antibody on western blots, we excluded its presence in the nucleus of Purkinje cells of patients with SCA2.

Although all three antibodies used here showed cytoplasmic staining, the SCA2-A and SCA2-B antibodies, which preferentially recognize full-length normal and mutated ataxin-2, yielded a more diffuse cytoplasmic staining, whereas the 1C2 antibody detected micro-aggregates. It has been suggested that truncated proteins may serve as a nidus for the formation of intranuclear aggregates[16] and in turn may recruit full-length proteins. The staining pattern observed in SCA2 brains is consistent with a similar mechanism for cytoplasmic aggregation. Although our studies emphasize the location of the initial toxic event in the cytoplasm, several questions regarding the initiation of cell dysfunction and eventual death remain unanswered. Because caspase cleavage appears to be important in cellular models of polyQ-induced apoptosis[40–42], mouse models using full-length cDNA constructs will provide the ideal basis for testing the importance of caspase cleavage *in vivo*. In human SCA2 brains, the abundance of the 42-kD ataxin-2 fragment appears to be increased compared with that of normal brains, although it is not yet known whether this truncation event is important for SCA2 pathogenesis.

Comparison of models. The ability of targeting transgene expression to a specific neuronal population facilitates evaluation of functional and anatomical consequences. The PcP2 promoter has now been used for the expression of ataxins 1, 2 and 3 with different results. Functional deficits and neuronal changes were only detected when ataxin-3 was severely truncated[31], although direct comparisons with other models may be difficult due to different expression levels of transgenes.

On the other hand, mice expressing ataxin-1[Q82] and ataxin-2[Q58] share similar functional and morphological features. Expression of ataxin-1 containing Q50 did not result in pathogenesis (H. Orr, pers. comm.), indicating the importance of the protein context for pathogenesis. When adjustments are made for different polyQ lengths, however, the similarity in the time course of pathological changes is striking. In both models, the functional impairment is mirrored by changes in the Purkinje-cell dendritic tree as visualized by altered calbindin-28K staining. Changes are dosage dependent and homozygous mice are affected significantly earlier than heterozygous animals[35,36,43]. Both ataxin models show evidence of neurodegeneration, although cell loss occurs much later than the onset of functional deficits. This pattern follows observations in human brains in that Purkinje cell atrophy in human hereditary ataxia begins with dendritic loss and then proceeds to the complete destruction of the cell body[44].

Despite these functional and morphological similarities between SCA1 and SCA2 transgenic lines, the site of the initiation of pathology appears to be different. In SCA1 nuclear localization is essential for pathogenesis, although intranuclear aggregation is not. We have now determined that neither normal nor mutant ataxin-2 acquire a nuclear localization. This holds true for mouse models, cultured cells (data not shown) and human Purkinje cells. We could also exclude the presence of fragments containing truncated polyQ in the nucleus. Although other investigators have detected occasional intranuclear aggregates in human SCA2 brains, these were never seen in Purkinje cells[30].

Previous results in cultured mouse and human neurons had suggested that ubiquitination and subsequent degradation by the proteasome machinery may be common to all polyQ proteins independent of their nuclear or cytoplasmic localization[8,23,45].

Ataxin-2 and possibly ataxin-6 appear to break this mold, at least with regard to detectable ubiquitination of aggregated or accumulated mutant proteins. In human SCA6 brains, ataxin-6 was not labelled by anti-ubiquitin antibodies[24]. In SCA2 human brains as well as in brains from transgenic mouse lines, no increase in the ubiquitination of ataxin-2 was detectable despite the presence of large amounts of immunoreactive ataxin-2 in the cytoplasm. In cultured cells, lactacystin-treated transfected cells did not produce ubiquitin-conjugated ataxin-2[58] complexes of high molecular weight, although the level of mutant ataxin-2 was increased in these cells. Ataxin-2[Q58] remained soluble, unlike ataxin-1 (ref. 23).

Expression studies of GFP linked to the p115 Golgi/ER transported protein led to the description of an aggresome complex that contained soluble, non-ubiquitinated proteins in its centre, although proteasome proteins and other chaperons were recruited into the aggresomes[46]. This contrasts with another class of aggresomes that involves the cytoplasmic aggregation and degradation of misfolded and ubiquitinated transmembrane proteins such as presenilin-1 or the cystic fibrosis transmembrane conductance regulator[47] (CFTR). Overexpression of the GFP–p115 chimaera caused incorrect Golgi localization, but with a normal ER-Golgi transport of the p115 protein. Our observations of non-Golgi localization of ataxin-2 with expanded polyQ repeats in cell culture (data not shown) and accumulation of ataxin-2 in human SCA2 neurons, together with the fact that wild-type ataxin-2 and its interactor (A2BP1) are both Golgi proteins, support this model[48].

Our study demonstrates in several distinct systems that intranuclear localization is not necessary for all classes of polyQ pathogenesis or for disease progression. The finding that cytoplasmic localization and microaggregation or accumulation of ataxin-2 cause Purkinje cell pathogenesis places SCA2 into the larger group of neurodegenerative diseases where protein aggregation occurs in the cytoplasm such as Parkinson and Alzheimer disease[49,50]. This group now appears to include one other polyQ protein, a subunit of the α-1A voltage-dependent calcium channel protein associated with SCA6 (ref. 24). Further studies need to investigate whether future treatments will need to be tailored to different mechanism of protein aggregation or whether common mechanisms can be identified despite these apparent differences.

## Methods

GFP fusion and transgenic plasmid constructs. We assembled a full-length *SCA2* cDNA including nt 145–4,481 (ref. 27) in the pBluescript vector with 22 or 58 CAG repeats. To generate ataxin-2 expression plasmids, we shuttled the full-length *SCA2* cDNA containing either the 22 or 58 CAG repeat into the pEGFPC2 (Clontech) or pcDNA vectors. These constructs were named pEGFP-SCA22, pEGFP-SCA58, pcDNA-SCA22 or pcDNA-SCA58.

We generated the transgenic construct replacing the β-galactosidase sequence from the pZ03-β-Gal plasmid, which contains the Pcp2/L7 promoter as well as untranslated and poly(A) sequences of *Pcp2* with the full-length SCA2 sequence[37]. The plasmid was a gift from H.T. Orr. We confirmed the correct recombinant plasmids by double-stranded sequencing. We named the transgenic recombinant plasmid pZ03SCA22 (22 CAG repeats) or pZ03SCA58 (58 CAG repeats). To linearize the transgenic construct, we digested the pZ03SCA22 and pZ03SCA58 plasmids with *Sal*I and *Aat*II to generate two bands of 2,188 and 6,451 bp. The 6,451-bp fragment was isolated in a sucrose gradient.

Transient expression of pEGFP-SCA2 constructs in 293T cells. To investigate ubiquitination of ataxin-2, we transfected 293T cells growing at 60% confluency in 100-mm Petri dishes with either pEGFP-SCA2 or pcDNA-SCA2 constructs (10 μg) containing either 22 or 58 CAG repeats. Transfected cells were grown overnight and then treated with culture medium with or without lactacystin (10 μM) for 24 h. We incubated cells with triple detergent buffer (0.5% SDS, 1% Triton-X100, 0.5% deoxycholate, 100 mM Tris-HCl, pH 8.0, 150 mM NaCl, and Sigma mammalian protease inhibitors cocktail) for 1 h in ice with occasional vortex. Protein extracts were centrifuged at maximum speed in an Eppendorf microfuge at 4 °C for 30 min and pellets resuspended in triple detergent buffer. Both protein extract and pellet suspension were stored at –70 °C. For western-blot analysis, we mixed 100 μg total protein extract per lane with SDS–PAGE sample buffer, and incubated for 2 h at 37 °C before loading into 4–15% SDS–PAGE gradient gel. Western blots were detected with SCA2A, 1C2 and ubiquitin antibodies.

Generation of transgenic mouse lines. We microinjected purified SCA2 transgenic fragments into pronuclei of the B6D2F1 mouse strain, a C57BL/6JxDBA/2J hybrid. Positive founders were backcrossed to wild type of the same hybrid strain. To determine the genotype of transgenic mice, tail DNAs were subjected to PCR using two primer pairs, one pair spanning the CAG-repeat region and the other pair spanning exons 16 and 17. Using this method, we identified 4 human mutant founder lines, Q58-5, Q58-11, Q58-5B and Q58-19 carrying 58 CAG repeats and 2 human wild-type lines, Q22-4 and Q22-5, carrying 22 CAG repeats. Only three Q58 lines, Q58-5B, Q58-11 and Q58-19, were able to produce offspring.

To determine transgene copy number, equal amounts of genomic DNAs from wild-type, Q22 and Q58 mice were digested with *Rsa*I and subjected to quantitative Southern-blot analysis after hybridization with an *SCA2* cDNA fragment common to both mouse and human (mouse exon 15).

CAG-repeat PCR analysis. At weaning age, a 1-cm piece of tail was cleaved from the animal and DNA was isolated using the Puregene DNA Isolation kit (Gentra System). After washing the precipitate was resuspended in TE buffer (100 μl). Using two primer pairs, we analysed tail DNA (50 ng) by PCR analysis to identify mice carrying the transgene. One primer pair, 1052A (5′–GCGTGCGAGCCGGTGTAT–3′) and 1190B (5′–CGGGCT TGCGGACATTG–3′), was a human-specific primer pair flanking the CAG-repeat region. Step-up PCR conditions were as follows: denaturation for 5 min at 95 °C, 5 cycles of denaturation at 95 °C for 1 min 30 s; annealing at 65 °C for 30 s, and extension at 72 °C for 1 min followed by 30 cycles of 95 °C, 1 min 30 s denaturation, 60 °C, 30 s annealing, and 72 °C, 1 min extension. This primer pair will generate a 145-bp fragment for the 22 CAG *SCA2* cDNA and a 258-bp fragment for the 58 *SCA2* cDNA. The second primer pair, A40 (5′–GGTTCCTTCT CATCCAACTG–3′) and 3′ STSB (5′–GATGTGTTCATGACT TTCAAGG–3′), flanks intron 16. At standard PCR conditions (35 cycles of 95 °C for 90 s denaturation, 60 °C for 30 s annealing, 72 °C for 4 min extension), the A40/3′STSB primer pair generates a 424-bp amplicon for the SCA2 transgene and a 1,424-bp amplicon for the endogenous gene (including intron 16).

RT–PCR and RNA isolation. Mouse cerebella were homogenized in Trisolve Reagent (Gibco) and total RNAs were isolated as described in the manufacturer's protocol. Total RNAs were selectively precipitated with 3.75 M LiCl/25 mM EDTA to remove trace genomic DNA contamination. The first-strand cDNA for RT–PCR was synthesized from total RNA (2 μg) using the Promega RT–PCR System. To compare the expression levels of the transgene from different lines, PCR was performed using primers 3014A (5′–TTACAGCCAAGTCTACTCTGAA–3′) and 3258B (5′–AGTCT GAACCCCTTGGGAA–3′), which span exon 15 and generate a 266-bp amplicon of the endogenous mouse transcript and a 260-bp amplicon from the transgene transcript. The primer pair 3014A/3258B amplifies the transgene slightly more efficiently due to two mismatches with the mouse sequence. To facilitate separation of the mouse and the human amplicons, we digested the PCR product with *Mse*I (New England BioLabs). Fragments were separated in 3% TBE MetaPhor agarose (MSI).

Clasping test. Mice were held by the tail for one minute. When the mouse folded both hindlegs close to the body, it received a score of 100. If only one leg was folded, it received a score of 50. Mice within one week of birth were grouped into a single test group.

Footprinting analysis. To measure stride length, we painted the left foot with red aqueous ink and the right foot with black ink and let the mouse run through a dark 40 cm×8 cm×6 cm (L×W×H) tunnel. The total stride length value obtained from each animal was an average of the stride length from the total number of steps produced by each leg. Hindleg footprints at 8 and 16 weeks were measured and compared between animals matched for age and weight.

Rotarod performance. To measure motor coordination and balance, we tested mice using Basile Rotarod treadmills (Stoeltingco). This test has been used to assess functional impairment in mice carrying SCA1 and huntingtin transgenes[18,22,36]. We placed mice on an accelerating rod with a rotating speed from 4 to 40 r.p.m. for a maximum of 10 min with a minimum intertrial interval of 15 min and recorded the time spent on the rod without falling. The duration of the test was 4 d with 4 individual trials per day.

Histological examination and immunohistochemistry. To determine whether Q58 transgenic mice exhibited Purkinje cell loss, we counted both calbindin-28K–positive and calbindin-28K–negative Purkinje cells from wild-type and Q58 transgenic mice at different ages. The percentage of surviving Purkinje cells were obtained by dividing the average number of Purkinje cells obtained from at least two different Q58 animals at the same age with the average number of Purkinje cells from seven wild-type animals.

We fixed human brain tissues obtained at necropsy in 10% formalin within 24 h of death and embedded selected samples in paraffin. Sections (6 μm) were cut and mounted onto Superplus microscopic slides (Fisher Scientific). The sections were rehydrated by rinsing twice at 5 min intervals in xylene, 100% ethanol, 95% ethanol and 70% ethanol. After deparaffinization, sections were treated with a protease cocktail, blocked with avidin/biotin and 3% normal goat serum. We incubated sections with 10–20 μg/ml of affinity-purified ataxin-2 antibodies overnight at 4 ºC. The other antibodies used were as follows: ubiquitin (Dako), 1C2 and calbindin D-28K (Chemicon). Primary antibodies were detected using the Vector rabbit ABC elite Peroxidase kit (Vector Labs), enhanced by DAB enhancer, and visualized with diaminobenzidine (DAB; Biomeda). We counterstained with aqueous haematoxylin (Xymed). Controls consisted of antibodies preabsorbed with 100 μM of the respective peptide and pre-immune sera at comparable concentrations (1/500). For direct comparison we processed all slides in a single batch to minimize variability.

**Acknowledgements**

*We thank A. Koeppen and M. Del Bigio for tissue samples from SCA2 patients; H. Orr for the pZ03-β-Gal expression vector with the Pcp2 promoter; C. Readhead and M. Schibler for assistance with transgenic mouse lines and confocal microscopy, respectively; T. Ho, A. Schlesinger and M. Dy for technical support; and D. Scoles and T.-R. Kiehl for critically reading the manuscript. This work was supported by the Carmen and Louis Warschaw Endowment for Neurology, F.R.I.E.N.D.s of Neurology, the National Ataxia Foundation, grant RO1-NS33123 (SMP) and a Long Term Disabled Scientist Supplement (DPH) from the National Institutes of Health.*

Received 1 June 1999; accepted 22 July 2000.

1. Orr, H.T. *et al.* Expansion of an unstable trinucleotide CAG repeat in spinocerebellar ataxia type 1. *Nature Genet*. **4**, 221–226 (1993).
2. Kawaguchi, Y. *et al.* CAG expansions in a novel gene for Machado-Joseph disease at chromosome 14q32.1. *Nature Genet* **8**, 221–228 (1994)
3. Zhuchenko, O. *et al.* Autosomal dominant cerebellar ataxia (SCA6) associated with small polyglutamine expansions in the α-1A-voltage-dependent calcium channel. *Nature Genet.* **15**, 62–69 (1997).
4. David, G. *et al.* Cloning of the SCA7 gene reveals a highly unstable CAG repeat expansion. *Nature Genet*. **17**, 65–70 (1997).
5. The Huntington's Disease Collaborative Research Group. A novel gene containing a trinucleotide repeat that is expanded and unstable on Huntington's disease chromosomes. *Cell* **72**, 971–983 (1993).
6. La Spada, A.R, Wilson, E.M., Lubahn, D.B., Harding, A.E. & Fischbeck, K.H. Androgen receptor gene mutations in X-linked spinal and bulbar muscular atrophy. *Nature* **352**, 77–79 (1991).
7. Koide, R. *et al*. Unstable expansion of CAG repeat in hereditary dentatorubral-pallidoluysian atrophy (DRPLA). *Nature Genet.* **6**, 9–13 (1994).
8. Cummings, C.J. *et al.* Chaperone suppression of aggregation and altered subcellular proteasome localization imply protein misfolding in SCA1. *Nature Genet*. **19**, 148–154 (1998).
9. Paulson, H.L. *et al.* Intranuclear inclusions of expanded polyglutamine protein in spinocerebellar ataxia type 3. *Neuron* **19**, 333–344 (1997).
10. Trottier, Y. *et al*. Heterogeneous intracellular localization and expression of ataxin-3. *Neurobiol. Dis.* **5**, 335–347 (1998).
11. Holmberg, M. *et al.* Spinocerebellar ataxia type 7 (SCA7): a neurodegenerative disorder with neuronal intranuclear inclusions. *Hum. Mol. Genet*. **7**, 913–918 (1998).
12. Igarashi, S. *et al.* Suppression of aggregate formation and apoptosis by transglutaminase inhibitors in cells expressing truncated DRPLA protein with an expanded polyglutamine stretch. *Nature Genet*. **18**, 111–117 (1998).
13. Davies, S.W. *et al.* Formation of neuronal intranuclear inclusions underlies the neurological dysfunction in mice transgenic for the HD mutation. *Cell* **90**, 537–548 (1997).
14. Martindale, D. *et al.* Length of huntingtin and its polyglutamine tract influences localization and frequency of intracellular aggregates. *Nature Genet*. **18**, 150–154 (1998).
15. Saudou, F., Finkbeiner, S., Devys, D. & Greenberg, M.E. Huntingtin acts in the nucleus to induce apoptosis but death does not correlate with the formation of intranuclear inclusions. *Cell* **95**, 55–66 (1998).
16. Scherzinger, E. *et al.* Huntingtin-encoded polyglutamine expansions form amyloid-like protein aggregates in vitro and in vivo. *Cell* **90**, 549–558 (1997).
17. Stenoien, D.L. *et al.* Polyglutamine-expanded androgen receptors form aggregates that sequester heat shock proteins, proteasome components and SRC-1, and are suppressed by the HDJ-2 chaperone. *Hum. Mol. Genet.* **8**, 731–741 (1999).
18. Reddy, P.H. *et al.* Behavioural abnormalities and selective neuronal loss in HD transgenic mice expressing mutated full-length *HD* cDNA. *Nature Genet*. **20**, 198–202 (1998).
19. Paulson, H.L. Protein fate in neurodegenerative proteinopathies: polyglutamine diseases join the (mis) fold. *Am. J. Hum. Genet.* **64**, 339–345 (1999).
20. Gutekunst, C.A. *et al.* Nuclear and neuropil aggregates in Huntington's disease: relationship to neuropathology. *J. Neurosci.* **19**, 2522–2534 (1999).
21. Kuemmerle, S. *et al.* Huntington aggregates may not predict neuronal death in Huntington's disease. *Ann. Neurol.* **46**, 842–849 (1999).
22. Klement, I.A. *et al.* Ataxin-1 nuclear localization and aggregation: role in polyglutamine-induced disease in SCA1 transgenic mice. *Cell* **95**, 41–53 (1998).
23. Cummings, C.J. *et al.* Mutation of the E6-AP ubiquitin ligase reduces nuclear inclusion frequency while accelerating polyglutamine-induced pathology in SCA1 mice. *Neuron* **24**, 879–892 (1999).
24. Ishikawa, K. *et al.* Abundant expression and cytoplasmic aggregations of [α]1A voltage-dependent calcium channel protein associated with neurodegeneration in spinocerebellar ataxia type 6. *Hum. Mol. Genet.* **8**, 1185–1193 (1999).
25. Nechiporuk, T. *et al.* The mouse SCA2 gene: cDNA sequence, alternative splicing, and protein expression. *Hum. Mol. Genet*. **7**, 1301–1309 (1998).
26. Imbert, G. *et al.* Cloning of the gene for spinocerebellar ataxia 2 reveals a locus with high sensitivity to expanded CAG/glutamine repeats. *Nature Genet.* **14**, 285–291 (1996).
27. Pulst, S.-M. *et al.* Moderate expansion of a normally biallelic trinucleotide repeat in spinocerebellar ataxia type 2. *Nature Genet.* **14**, 269–276 (1996).
28. Sanpei, K. *et al.* Identification of the spinocerebellar ataxia type 2 gene using a direct identification of repeat expansion and cloning technique, DIRECT. *Nature Genet.* **14**, 277–284 (1996).
29. Huynh, D.P., Del Bigio, M.R., Ho, D.H. & Pulst, S.-M. Expression of ataxin-2 in brains from normal individuals and patients with Alzheimer's disease and spinocerebellar ataxia 2. *Ann. Neurol.* **45**, 232–241 (1999).
30. Koyano, S. *et al.* Neuronal intranuclear inclusions in spinocerebellar ataxia type 2: triple-labeling immunofluorescent study. *Neurosci. Lett.* **273**, 117–120 (1999).
31. Ikeda, H. *et al.* Expanded polyglutamine in the Machado-Joseph disease protein induces cell death *in vitro* and *in vivo*. *Nature Genet.* **13**, 196–202 (1996).
32. Mangiarini, L. *et al.* Exon 1 of the HD gene with an expanded CAG repeat is sufficient to cause a progressive neurological phenotype in transgenic mice. *Cell* **87**, 493–506 (1996).
33. Mangiarini, L. *et al.* Instability of highly expanded CAG repeats in mice transgenic for the Huntington's disease mutation. *Nature Genet.* **15**, 197–200 (1997).
34. Davies, S.W. *et al*. From neuronal inclusions to neurodegeneration: neuropathological investigation of a transgenic mouse model of Huntington's disease. *Phil. Trans. R. Soc. Lond. B Biol. Sci.* **354**, 981–989 (1999).
35. Burright, E.N. *et al.* SCA1 transgenic mice: a model for neurodegeneration caused by an expanded CAG trinucleotide repeat. *Cell* **82**, 937–948 (1995).
36. Clark, H.B. *et al.* Purkinje cell expression of a mutant allele of SCA1 in transgenic mice leads to disparate effects on motor behaviors, followed by a progressive cerebellar dysfunction and histological alterations. *J. Neurosci.* **17**, 7385–7395 (1997).
37. Vandaele, S. *et al.* Purkinje cell protein-2 regulatory regions and transgene expression in cerebellar compartments. *Genes Dev.* **5**, 1136–1148 (1991).
38. Paulson, H.L. *et al.* Intranuclear inclusions of expanded polyglutamine protein in spinocerebellar ataxia type 3. *Neuron* **19**, 333–344 (1997).
39. Hodgson, J.G. *et al.* A YAC mouse model for Huntington's disease with full-length mutant huntingtin, cytoplasmic toxicity, and selectivity striatal neurodegeneration. *Neuron* **23**, 181–192 (1999).
40. Sanchez, I. *et al.* Caspase-8 is required for cell death induced by expanded polyglutamine repeats. *Neuron* **22**, 623–633 (1999).
41. Kim, M. *et al.* Mutant huntingtin expression in clonal striatal cells: dissociation of inclusion formation and neuronal survival by caspase inhibition. *J. Neurosci.* **19**, 964–973 (1999).
42. Wellington, C.L. *et al.* Caspase cleavage of gene products associated with triplet expansion disorders generates truncated fragments containing the polyglutamine tract. *J. Biol. Chem.* **273**, 9158–9167 (1998).
43. Vig, P.J. *et al.* Reduced immunoreactivity to calcium-binding proteins in Purkinje cells precedes onset of ataxia in spinocerebellar ataxia-1 transgenic mice. *Neurology* **50**, 106–113 (1998).
44. Koeppen, A.H. The Purkinje cell and its afferents in human hereditary ataxia. *J. Neuropathol. Exp. Neurol.* **50**, 505–514 (1991).
45. Chai, Y. *et al*. Evidence for proteasome involvement in polyglutamine disease: localization to nuclear inclusions in SCA3/MJD and suppression of polyglutamine aggregation *in vitro*. *Hum. Mol. Genet.* **8**, 673–682 (1999).
46. Garcia-Mata, R. *et al*. Characterization and dynamics of aggresome formation by a cytosolic GFP-chimera. *J. Cell Biol.* **146**, 1239–1254 (1999).
47. Johnston, J.A., Ward, C.L. & Kopito, R.R. Aggresomes: a cellular response to misfolded proteins. *J. Cell Biol.* **143**, 1883–1898 (1998).
48. Shibata, H., Huynh, D.P. & Pulst S.-M. A novel protein with RNA binding motifs interacts with ataxin-2. *Hum. Mol. Genet.* **9**, 130–1313 (2000).
49. Mezey, E. *et al.* α synuclein is present in Lewy bodies in sporadic Parkinson's disease. *Mol. Psychiatry* **3**, 493–499 (1998).
50. Lippa, C.F. *et al.* Lewy bodies contain altered α-synuclein in brains of many familial Alzheimer's disease patients with mutations in presenilin and amyloid precursor protein genes. *Am. J. Pathol.* **153**, 1365–1370 (1998).